Electronic Supplementary Material (ESI) for New Journal of Chemistry.

NJC

Supporting Information

Mixed-halides copper-based perovskite $R_2Cu(Cl/Br)_4$ with different organic cations for reversible thermochromism

Amr Elattar,[*a, b] Kosei Tsutsumi,[a] Hiroo Suzuki,[a] Takeshi Nishikawa,[a] Aung Ko Ko Kyaw,[c] and Yasuhiko Hayashi[a]

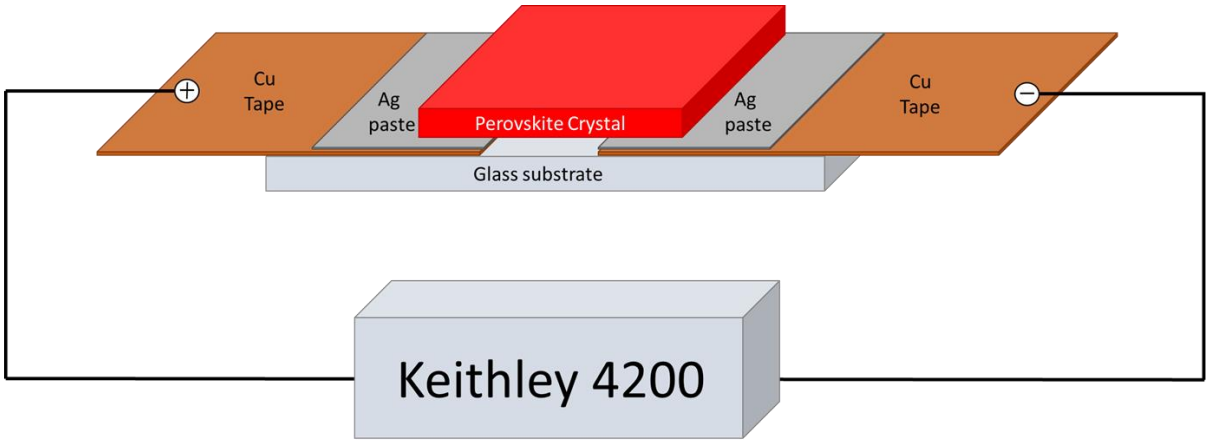

Fig. S1 Representation of temperature-dependent conductivity measurements.

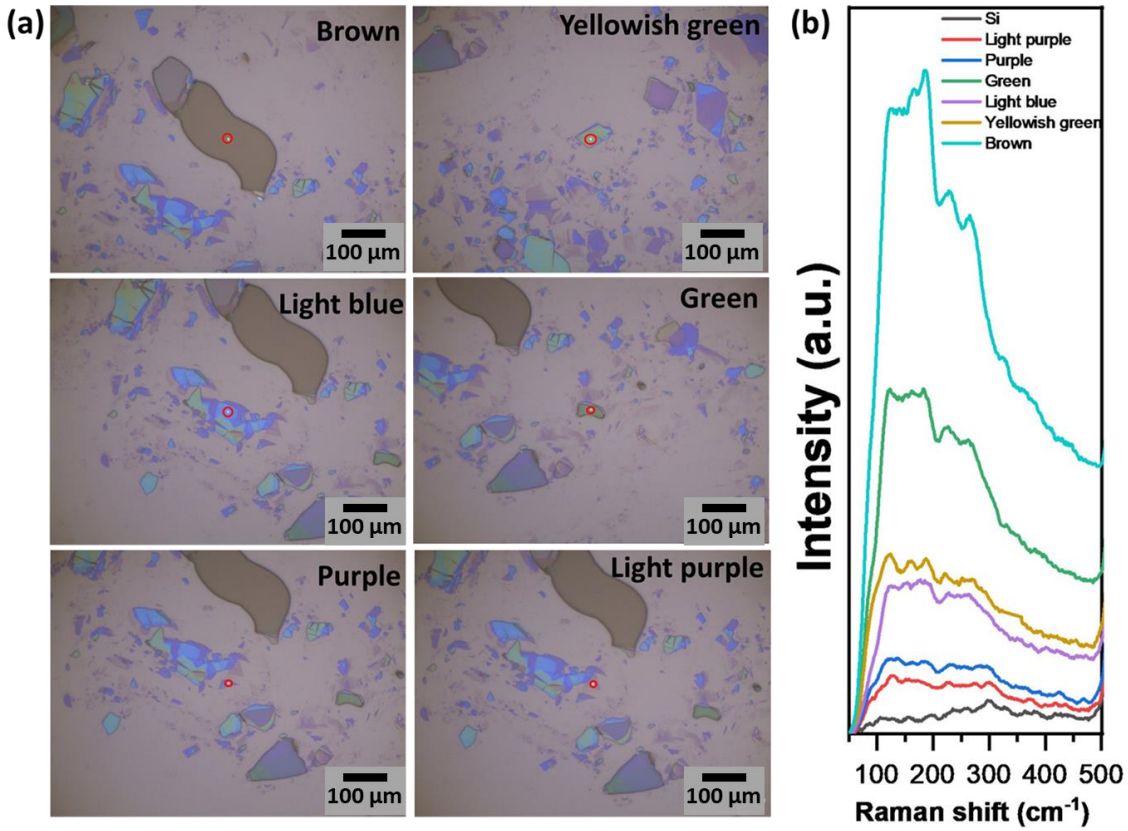

Fig. S2 Exfoliation effect (a) Optical microscopic images of different mechanically exfoliated **$HA_2Cu(Cl/Br)_4$** flakes, scale bar (100 µm). (b) Raman spectra of exfoliated flakes in the range of 50–500 cm^{-1}.

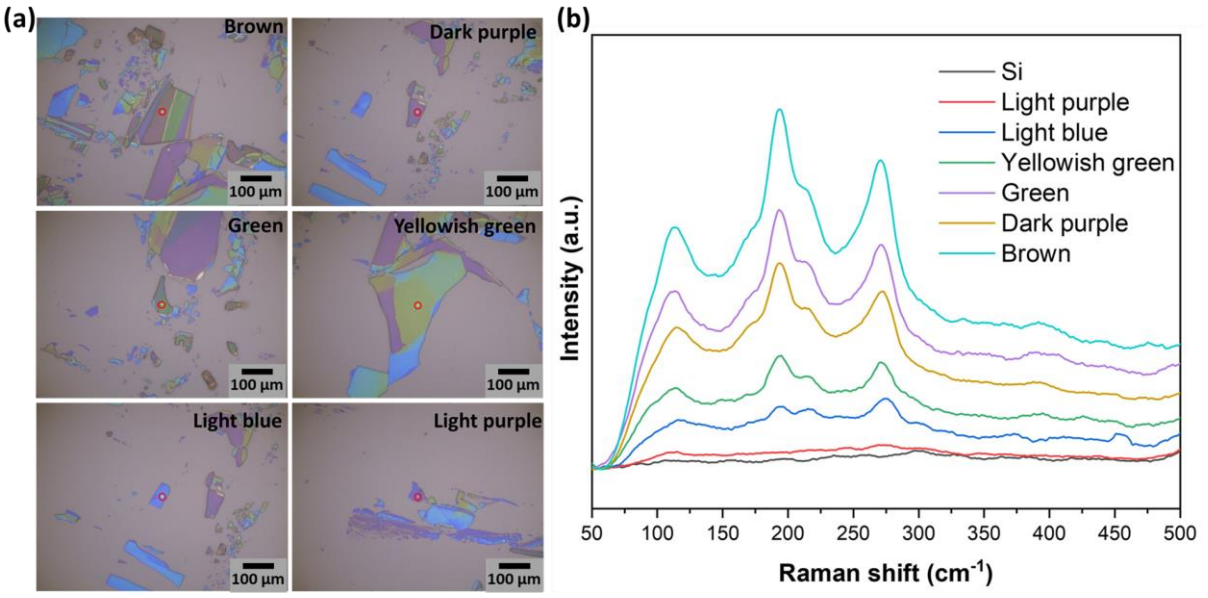

Fig. S3 Exfoliation effect (a) Optical microscopic images of different mechanically exfoliated **$MA_2Cu(Cl/Br)_4$** flakes, scale bar (100 μm). (b) Raman spectra of exfoliated flakes in the range of 50–500 cm^{-1}.

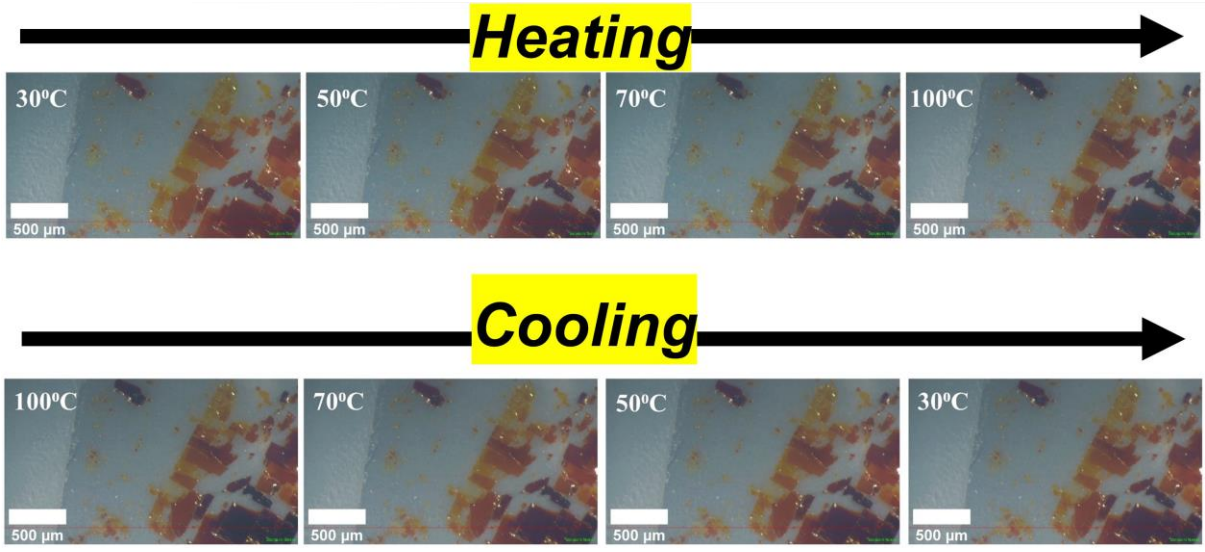

Fig. S4 Temperature-induced color change of MA perovskite crystal flakes with heating and cooling cycles, respectively.

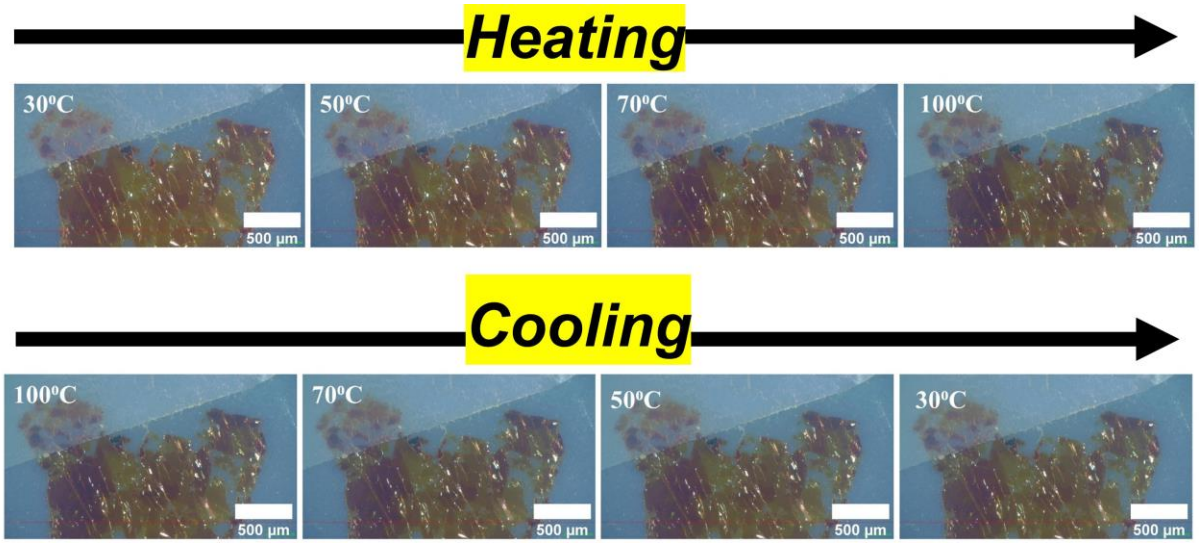

Fig. S5 Temperature-induced color change of BA perovskite crystal flakes with heating and cooling cycles, respectively.

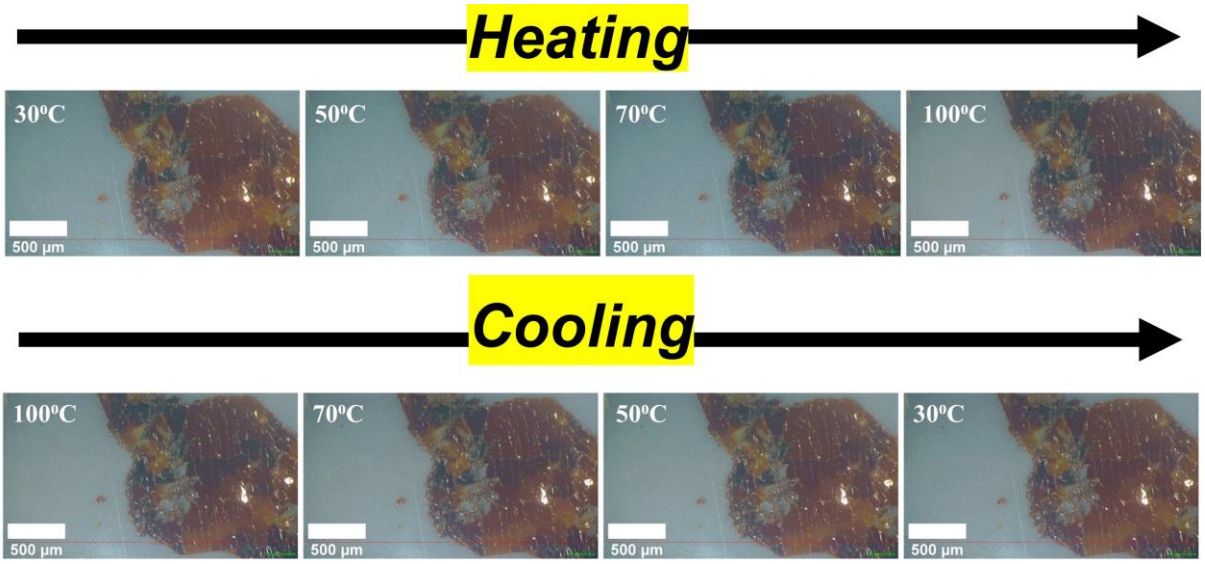

Fig. S6 Temperature-induced color change of HA perovskite crystal flakes with heating and cooling cycles, respectively.

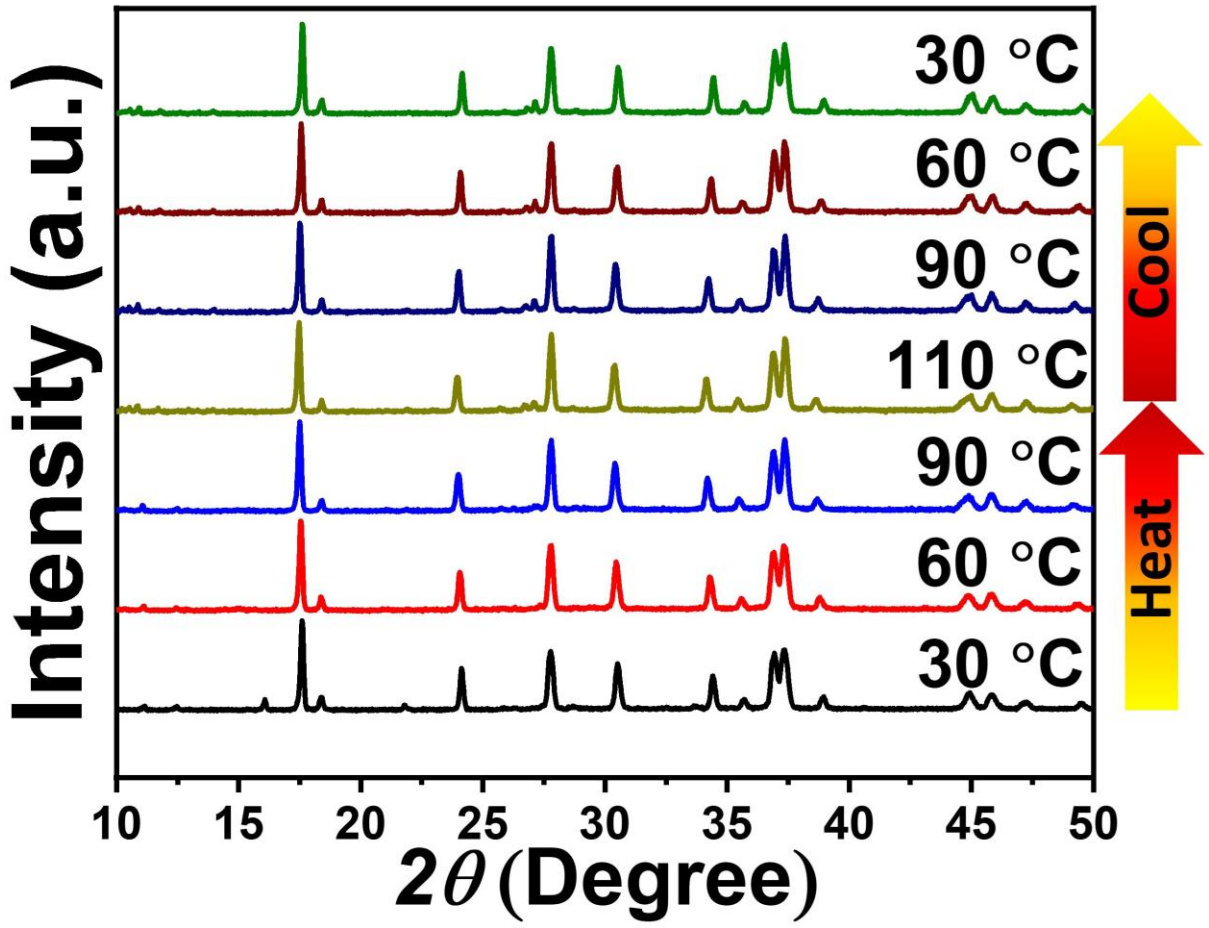

Fig. S7 Temperature dependent XRD of MA perovskite.

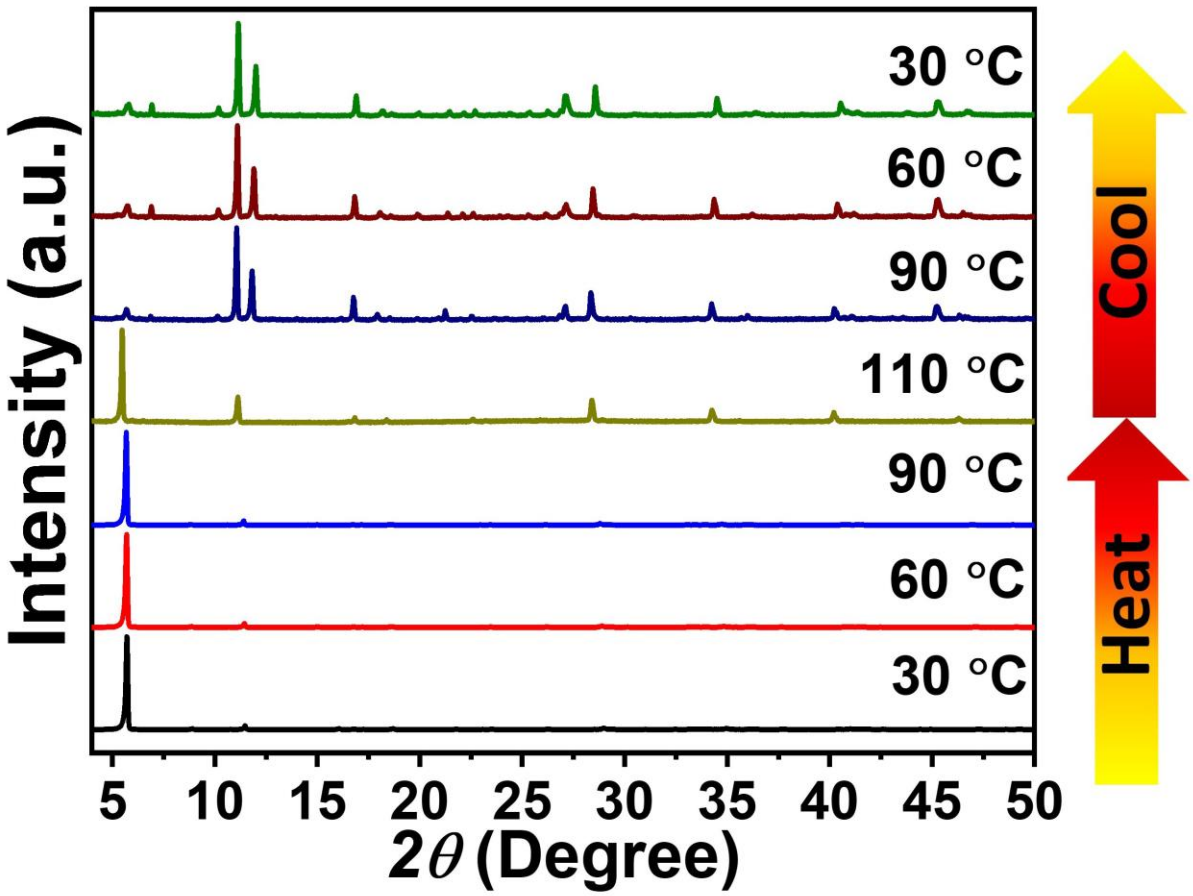

Fig. S8 Temperature dependent XRD of BA perovskite.

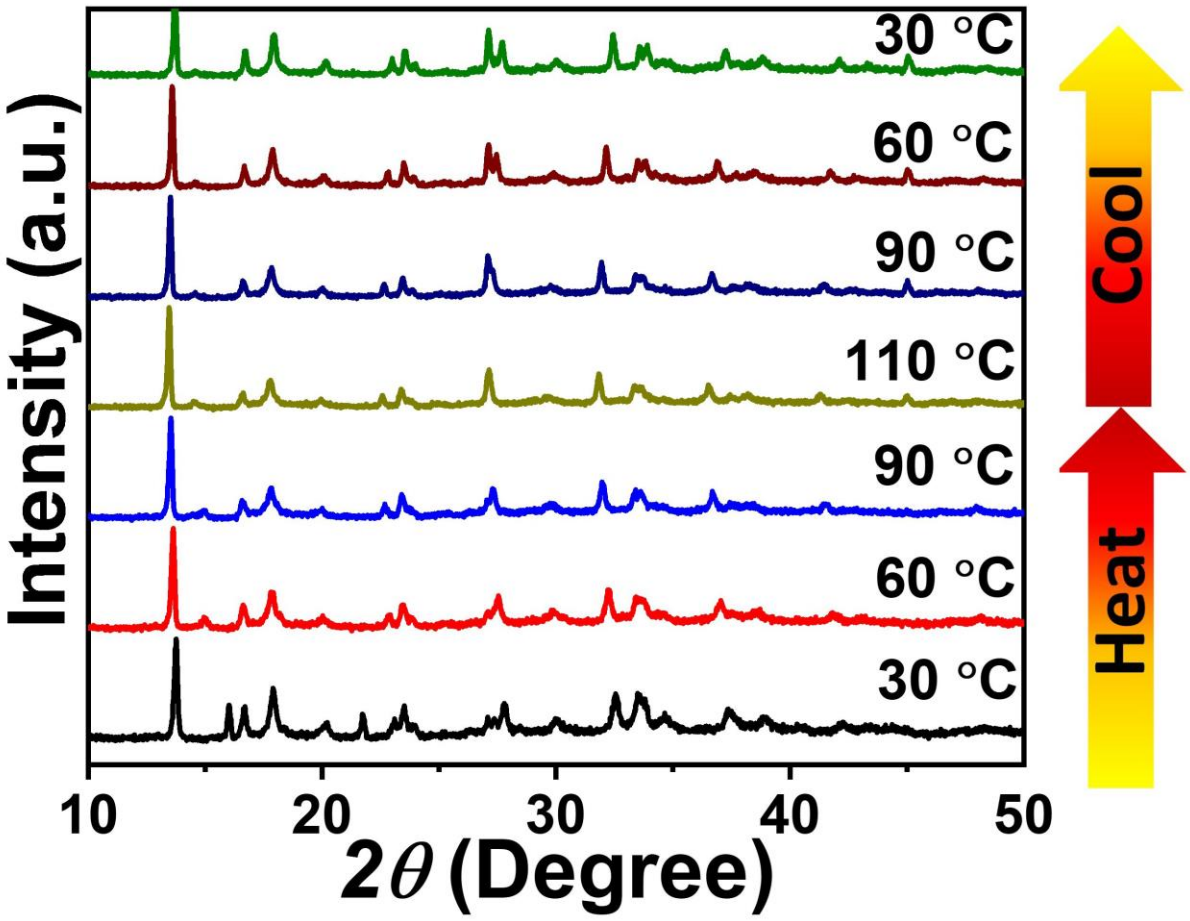

Fig. S9 Temperature dependent XRD of HA perovskite.

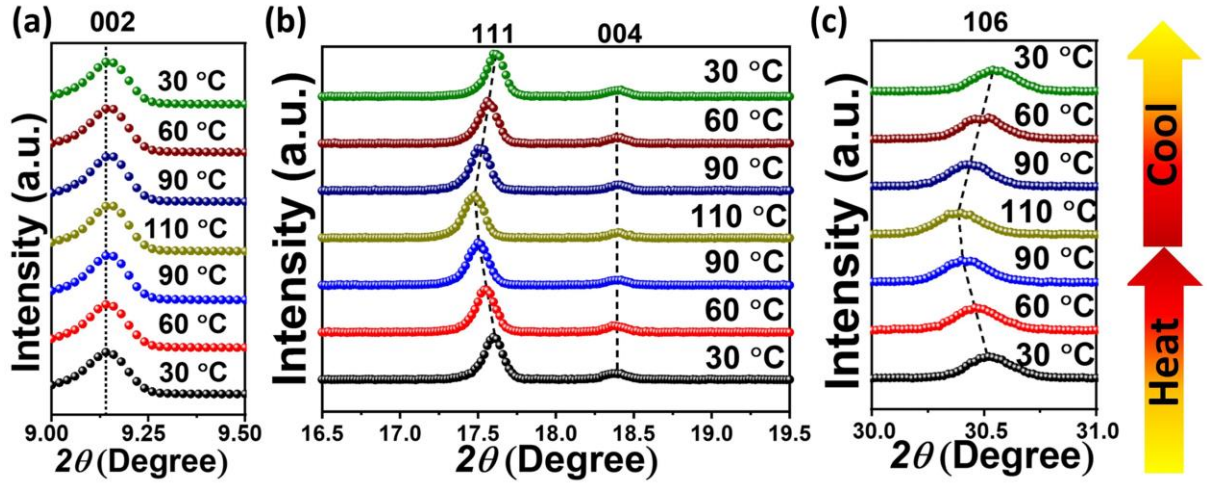

Fig. S10 Temperature dependent XRD of MA perovskite: Enlarged peaks of 002 peak(a), 111 and 004 peaks (b), and 106 peak (c).

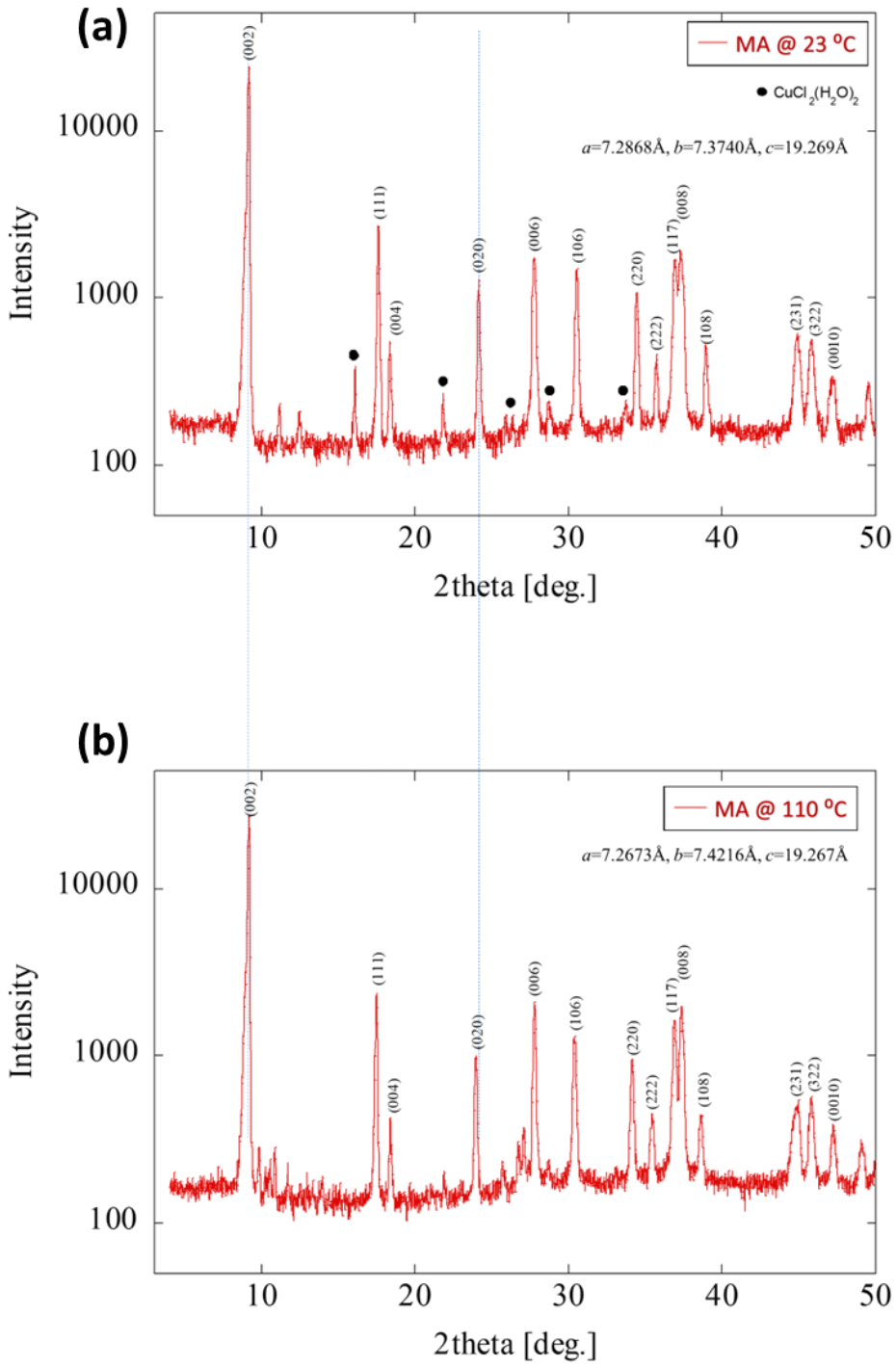

Fig. S11 XRD with lattice constant simulatiom of MA perovskite at 23 °C (a) and at 110 °C.

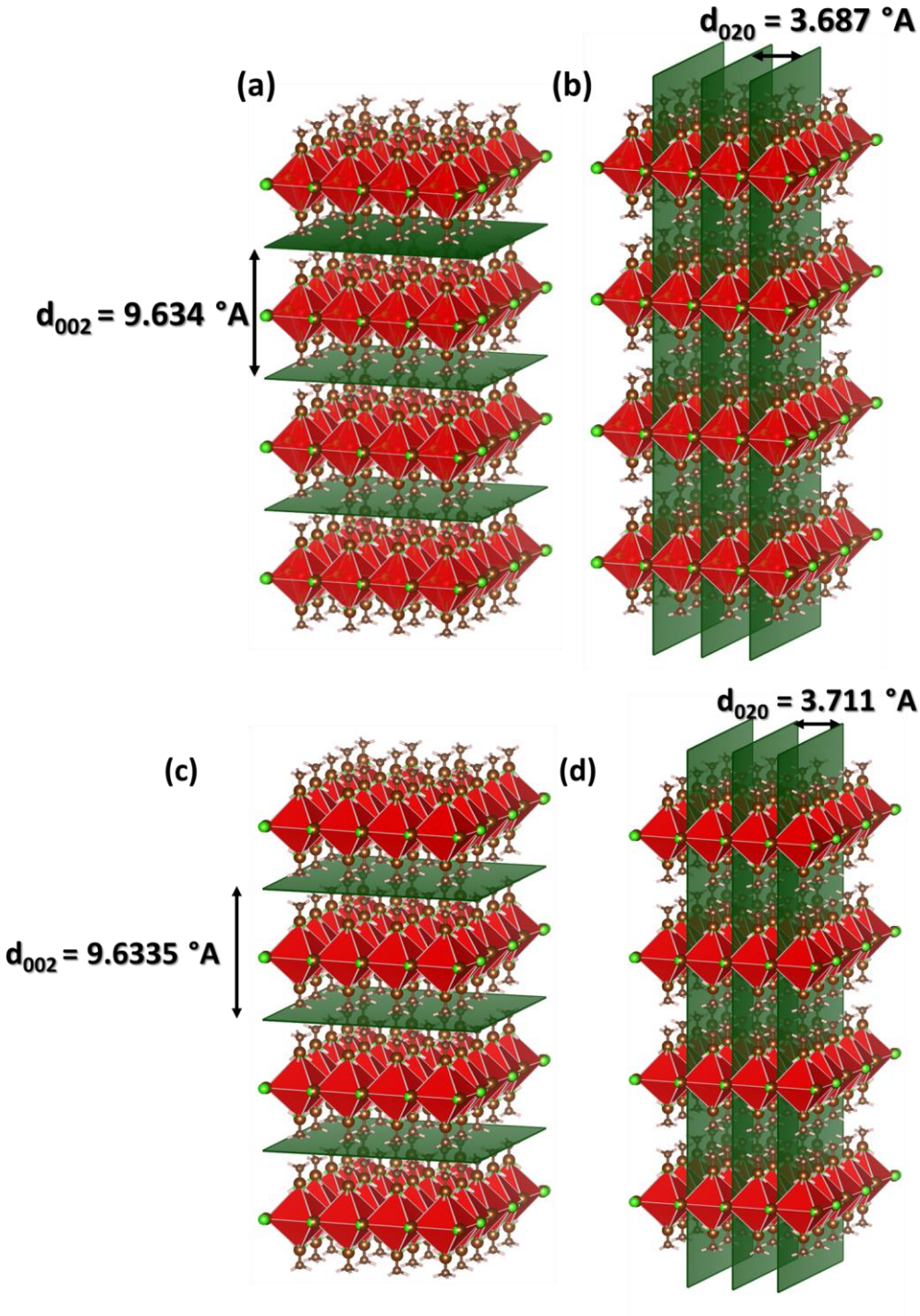

Fig. S12 Simulated Crystal structure of MA perovskite with lattice constant simulatiom of MA perovskite at 23 ^{o}C (a,b) and at 110 ^{o}C (c, d).

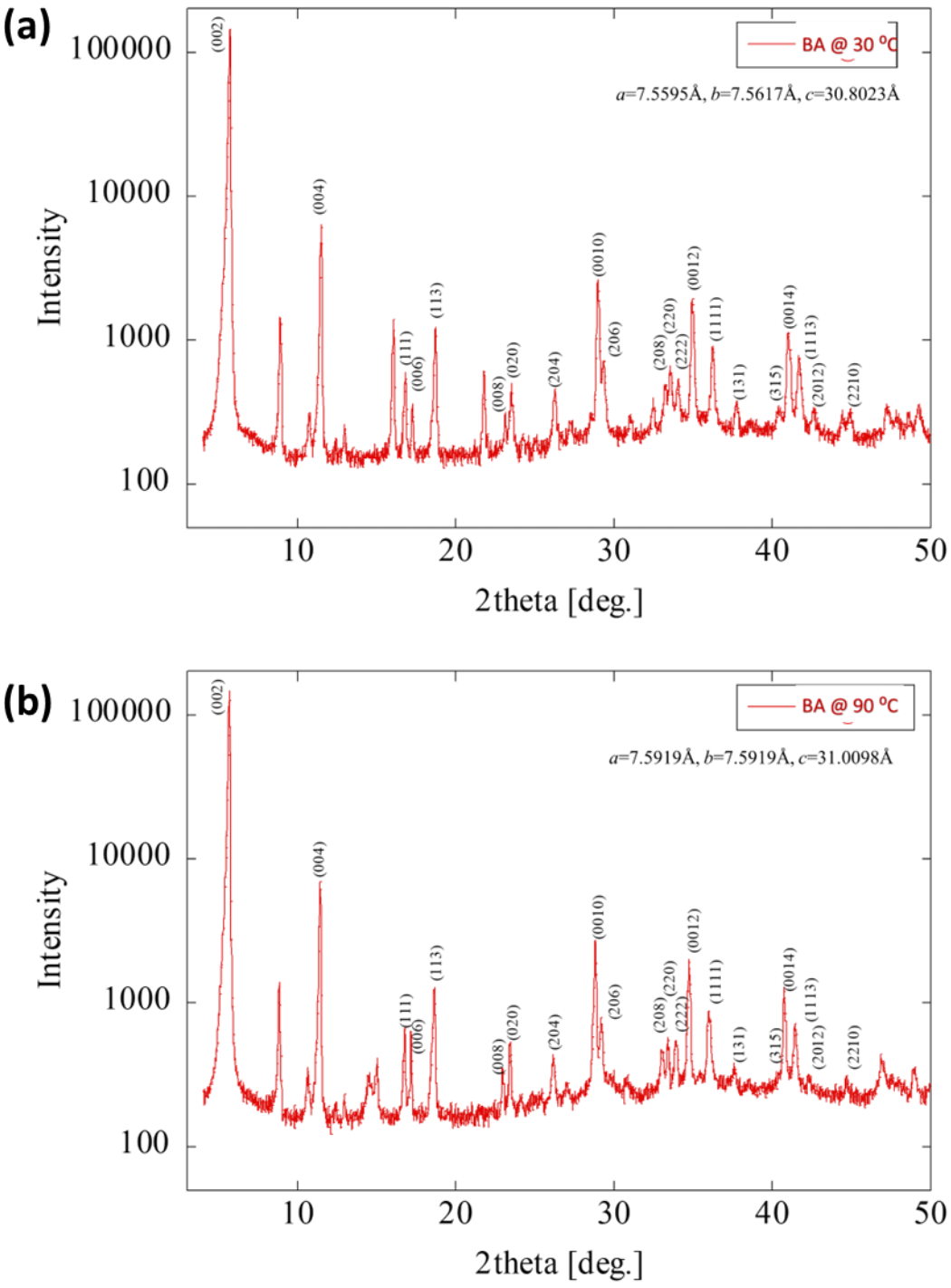

Fig. S13 XRD with lattice constant simulatiom of BA perovskite at 30 °C (a) and at 90 °C (b).

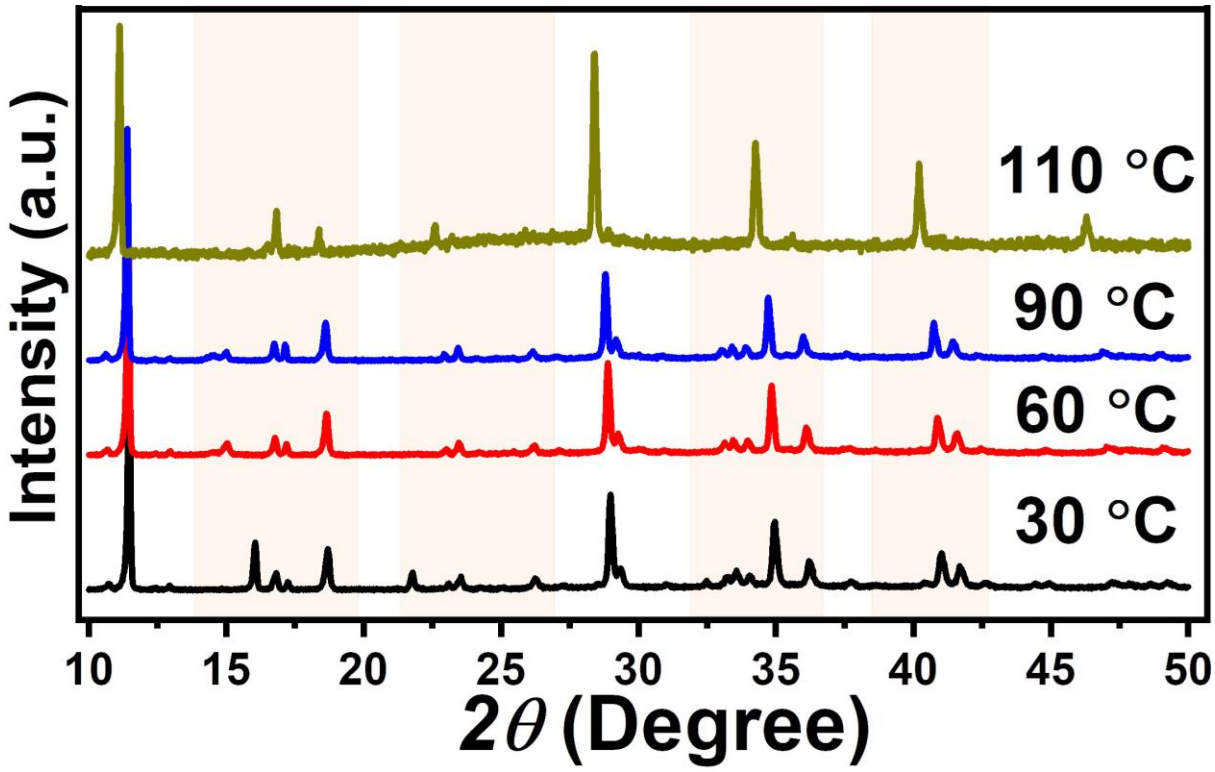

Fig. S14 Temperature dependent XRD (Enlarged peaks) of BA perovskite.

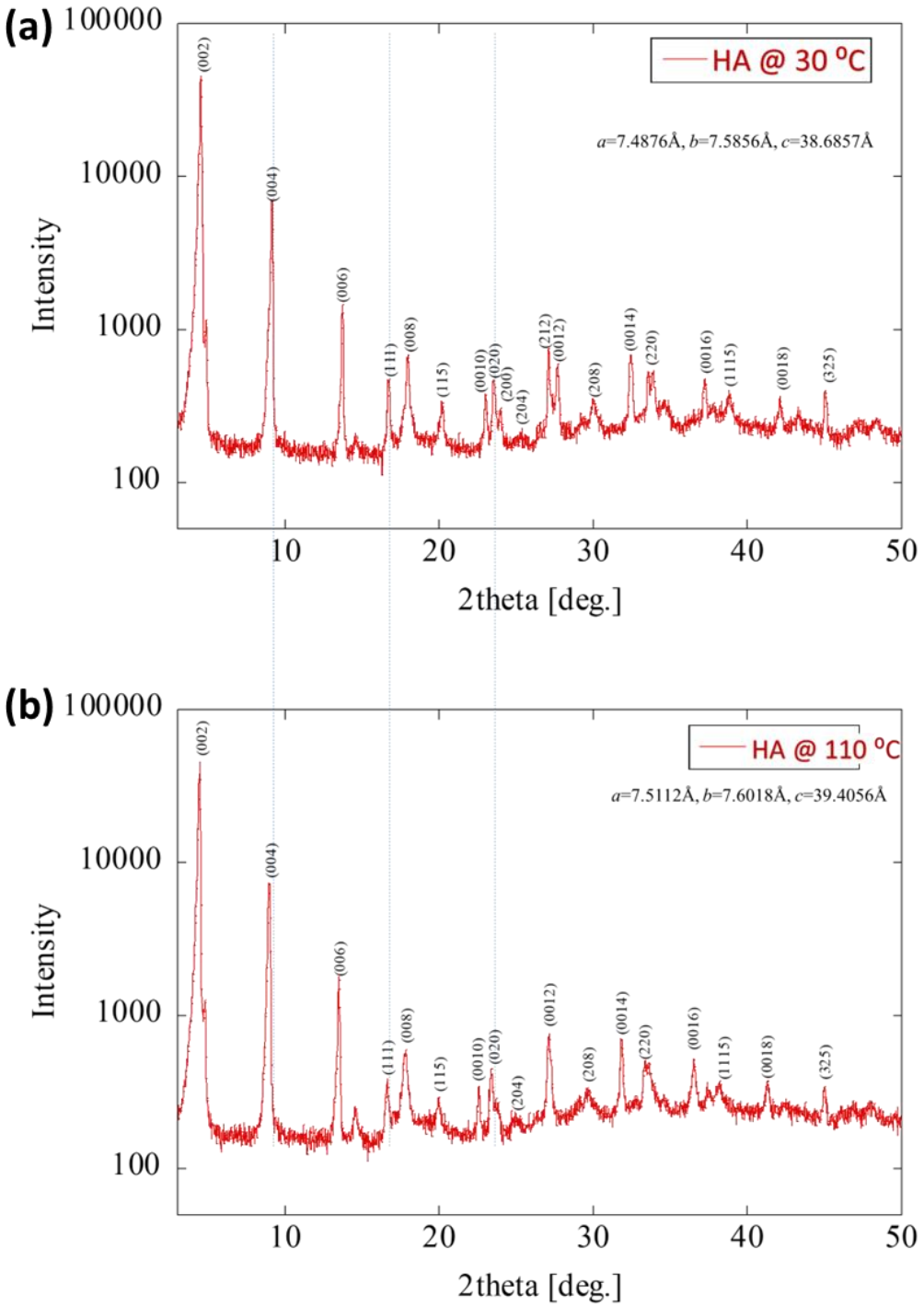

Fig. S15 XRD with lattice constant simulatiom of HA perovskite at 30 °C (a) and at 110 °C (b).

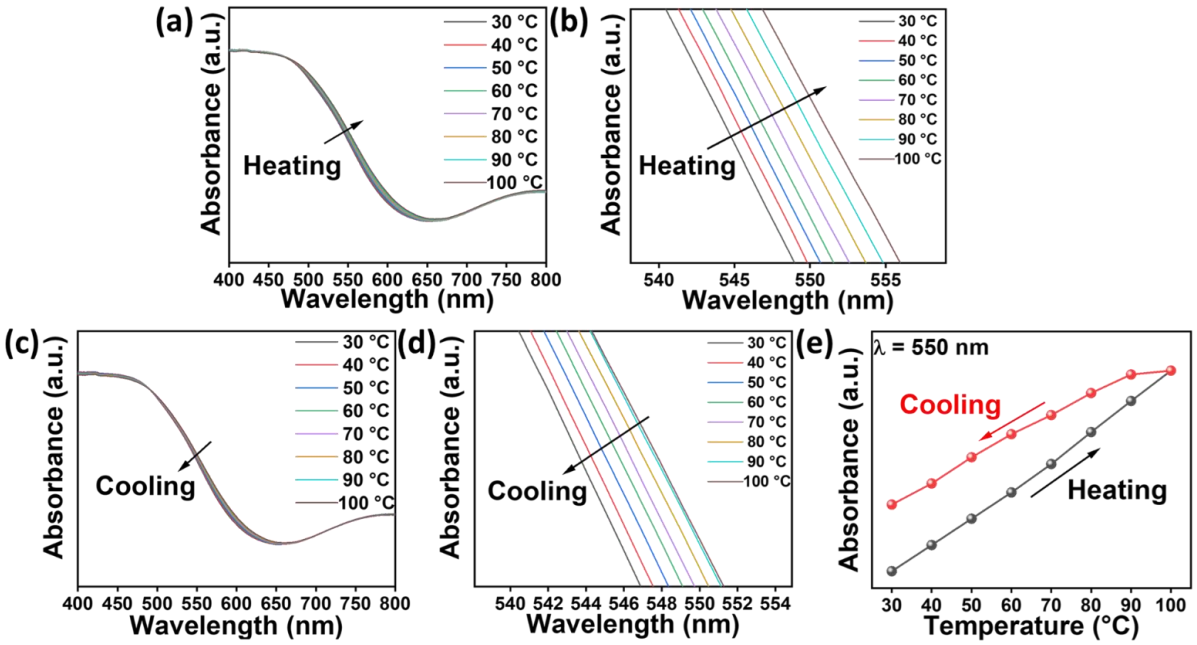

Fig. S16 Temperature dependence of absorption spectra of **$MA_2Cu(Cl/Br)_4$** crystal for heating (a, b) / cooling cycle (c, d) with hysteresis loops (e).

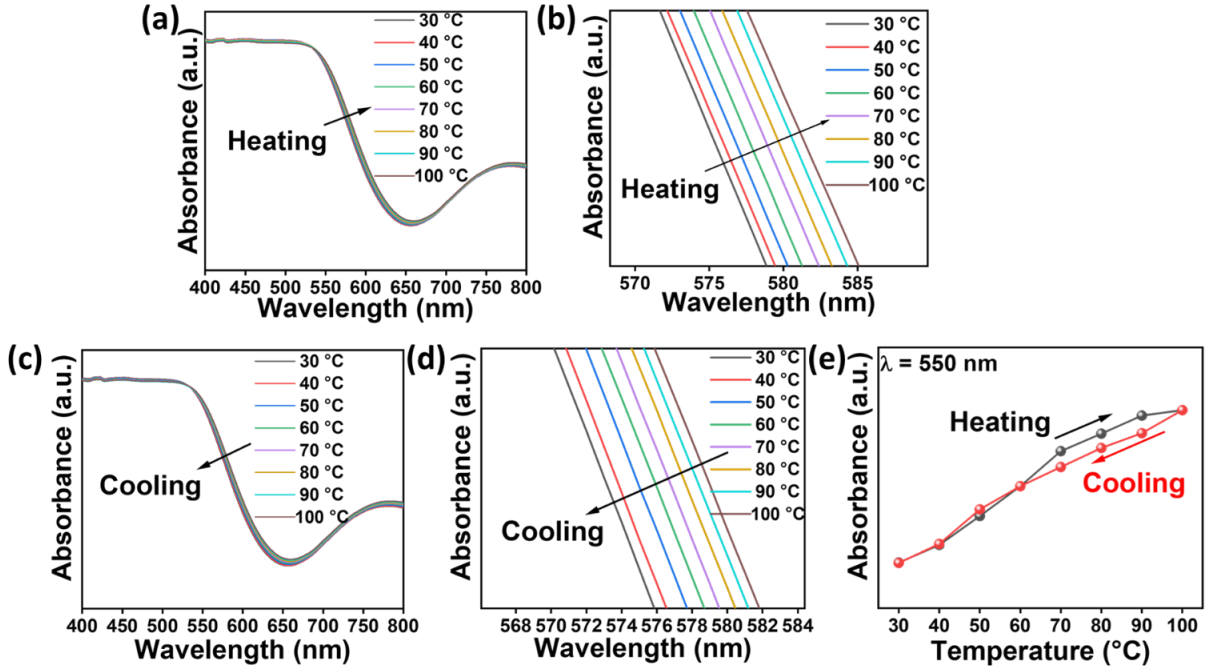

Fig. S17 Temperature dependence of absorption spectra of **$HA_2Cu(Cl/Br)_4$** crystal for heating (a, b) / cooling cycle (c, d) with hysteresis loops (e).

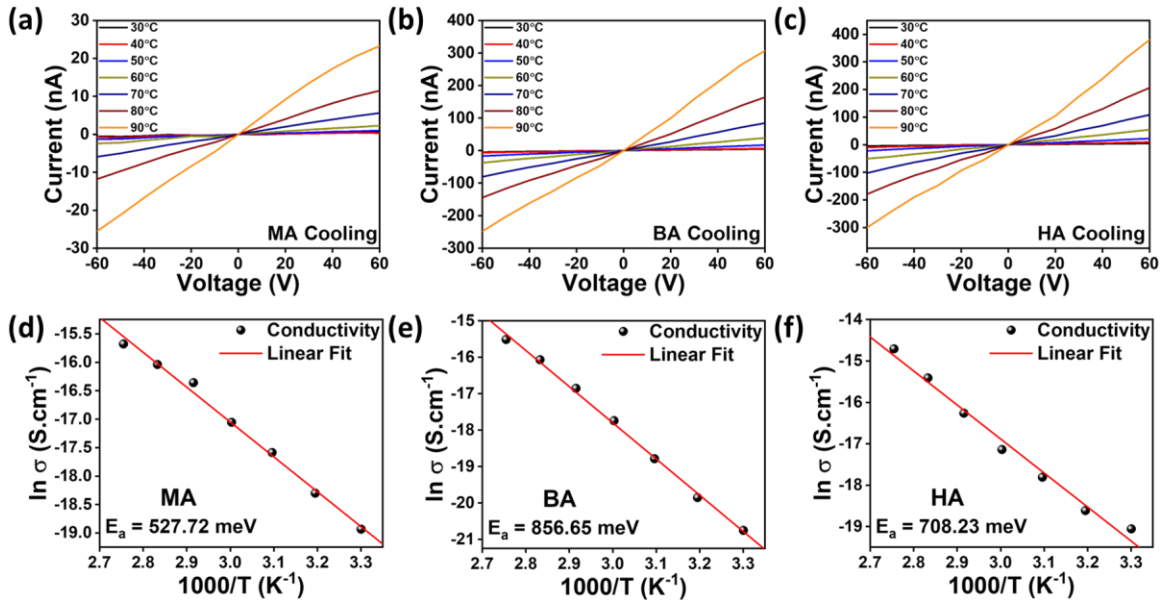

Fig. S18 Temperature dependent current/voltage curves of $MA_2Cu(Cl/Br)_4$ (a), $BA_2Cu(Cl/Br)_4$ (b), and $HA_2Cu(Cl/Br)_4$ (c) between −60 V and 60 V bias. Arrhenius fit of the natural logarithm of conductivity versus inverse temperature of $MA_2Cu(Cl/Br)_4$ (d), $BA_2Cu(Cl/Br)_4$ (e), and $HA_2Cu(Cl/Br)_4$ (f).

Table S1 Energy dispersive spectroscopy (EDS) data for determination of the organic cation content of perovskite crystals.

Perovskite	%Cl	%Br	Cl fraction	Br fraction
$MA_2Cu(Cl/Br)_4$	26.78	13.55	2.6	1.4
$BA_2Cu(Cl/Br)_4$	14.55	9.37	2.5	1.5
$HA_2Cu(Cl/Br)_4$	12.34	7.41	2.5	1.5